Two dimensional periodic array of reflection centers on electrodes in SAW resonators

Jiman Yoon, Markus Mayer, Thomas Ebner, Karl Wagner, Achim Wixforth

Angaben zur Veröffentlichung / Publication details:

Yoon, Jiman, Markus Mayer, Thomas Ebner, Karl Wagner, and Achim Wixforth. 2012. "Two dimensional periodic array of reflection centers on electrodes in SAW resonators." In *2012 IEEE International Ultrasonics Symposium, Dresden, Germany, 7-10 October 2012*, 1–4. Piscataway, NJ: IEEE. https://doi.org/10.1109/ultsym.2012.0451.

10.1109/ULTSYM.2012.0451

Two Dimensional Periodic Array of Reflection Centers on Electrodes in SAW Resonators

Jiman Yoon[1,2], M. Mayer[2], T. Ebner[2], K. Wagner[2], A. Wixforth[1]

[1]*Experimental Physics I, University of Augsburg*
Universitätsstr. 1 D-86159 Augsburg, Germany
ji.man.yoon@student.uni-augsburg.de
achim.wixforth@physik.uni-augsburg.de
[2]*TDK/EPCOS AG*
Munich, Germany
[2]thomas.ebner@epcos.com

Abstract—**Periodic arrays of metallic patches on the electrodes of a "Rayleigh-type SAW resonator" are investigated to suppress undesired modes above resonance frequency. Both, the metallization ratio(η_t) and the period(P_L) of the patches in transversal direction, were varied. Simulations were performed employing the well established 2D P-matrix model.**

A well-designed periodic array is capable to suppress all transversal modes within the frequency band for $k_y = \left[0, \frac{\pi}{P_T}\right]$. By evaluation of the overlap integral of the excitation and mode profile, and consequently, the analysis of the single mode contribution to the excitation strength, it is demonstrated that higher modes are responsible for remaining spurious peaks in the resonator's frequency response.

The analysis of the contribution of the transversal modes to the admittance provides insight how the $\Delta v/v$ waveguide, formed by the areas with and without patches, can be engineered to suppress bound and leaky continuum modes.

***Keywords*— Periodic Array, Spurious Mode, Waveguide, Excitation Strength**

I. Introduction

SAW resonator filters are widely used in the field of telecommunications [1], [2]. Due to the finite aperture of the acoustic track of a resonator, various diffraction effects may occur. Acoustic tracks forming good waveguides show transversal modes propagating under certain angles with respect to the main propagation direction giving rise to undesired peaks in the pass- and the stopband [3], [4]. This inherent attribute deteriorates the characteristics of the frequency response in SAW filters. Various methods have been reported to suppress transversal modes. Aperture weighting can be used to smoothen the transversal mode peaks but this requires additional space and the transversal modes are still excited and the corresponding loss is still existing. A "Piston Mode Design" fully suppresses all but the fundamental mode [5]. Recently, so-called "Phononic Crystals" have been proposed for mode suppression in SAW devices [6]. A perfect 2D phononic crystal has a stopband in all directions of the filter surface. Whereas phononic crystals on a macroscopic scale were successfully fabricated, they are not easy to be realized on the micrometer scale [7]. In this work,

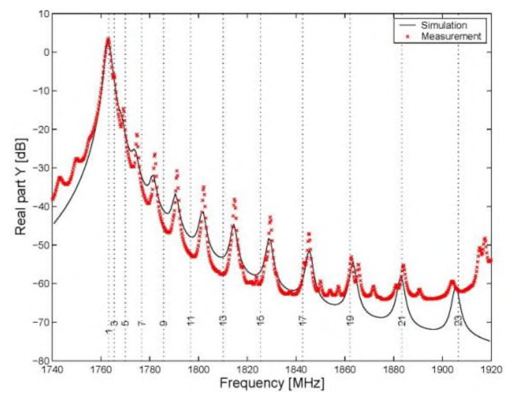

Fig. 1 Y_{12} of a reference one port resonator, Simulation (black) and measurement (red) are in excellent agreement if model parameters for simulation are accurate.

we investigated 2D periodic arrays of metallic patches on the electrodes in a Rayleigh-type SAW resonator. Both, the metallization ratio and the period of the patches in transversal direction were varied and the resulting effect on the mode spectrum was investigated.

Simulations were performed employing the well established 2D P-matrix model. The 2D P-matrix model describes waveguiding and reflection in SAW filters by discretizing acoustic tracks into longitudinal and transversal sections, where free waveguide propagation is assumed within a longitudinal section and reflection is assumed to be concentrated at section boundaries [8], [9], [10].

In Section II, the method of analysis is introduced as well as the principle of mode suppression. In section III, the modal decomposition of the excitation strength is dealt with to analyse spurious mode suppression.

II. Approach

It is well known that the excitation of the transversal spurious modes originates from the different shapes of the transversal electroacoustic transduction profile and the fundamental symmetric mode [5], [11]. The former is usually rectangular-like, while the latter differs from case to case. As

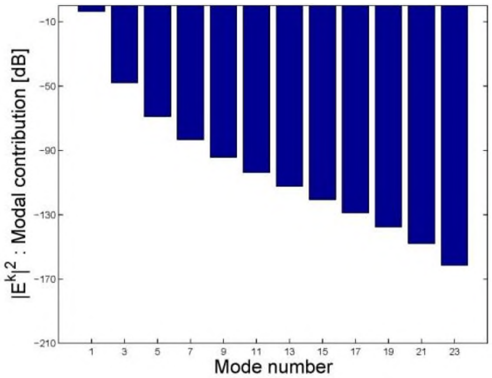

Fig. 2 Excitation strengths of transversal modes. Only symmetric modes are shown on the bar plot since the anti symmetric mode cancel out.

mentioned in the previous section, popular methods to control spurious modes are "Aperture Weighting", where the average excitation profile resembles the fundamental mode and a "Piston Mode device", where a rectangular fundamental mode, ψ_1, is enforced [11].

In principle, the 2D P-matrix method allows to represent the conductance as the sum of modal contributions [9]. However, this method is a bit complicated to be interpreted directly. A simple scheme to guess the position of peaks originating from higher transversal modes is the assumption of sinusoidal modes in a velocity profile with infinitely high walls, [4], where the parabolic approximation is assumed and mode coupling by reflection is not considered, i.e.,

$$k_x^2 + k_y^2(1+\gamma) = k_0^2, \tag{1}$$

where $k_x = \frac{\pi}{p_L}$, the wave number of longitudinal periodicity (p_L) of active fingers, $k_y = \frac{\pi}{A} \cdot m$, and A is the aperture of the waveguide. γ is the anisotropy coefficient and is assumed to be constant. $k_0 = \frac{2\pi f_m}{v_0}$ is the wave number in x-direction, where v_0 is the velocity in x-direction and f_m is the frequency of mode m . By solving the above equation for f_m we obtain;

$$f_m = f_0\sqrt{1+\left(\frac{p_L m}{A}\right)^2(1+\gamma)}\,, \tag{2}$$

where $f_0 = \frac{v_0}{2p_L}$ is the resonance frequency for the one dimensional case. Since the coupling is neglected in this simple approximation, deviations from the peak positions become larger the higher the mode numbers are (Fig 1). For the low lying transversal modes, contrarily, the positions of the peaks are predicted quite precisely.

To investigate the symmetric modal contribution of the observed peaks, we have to look at the excitation strength of each mode. The excitation strength of the kth mode is the scalar product of excitation profile and mode profile over the transversal direction [11], i.e.,

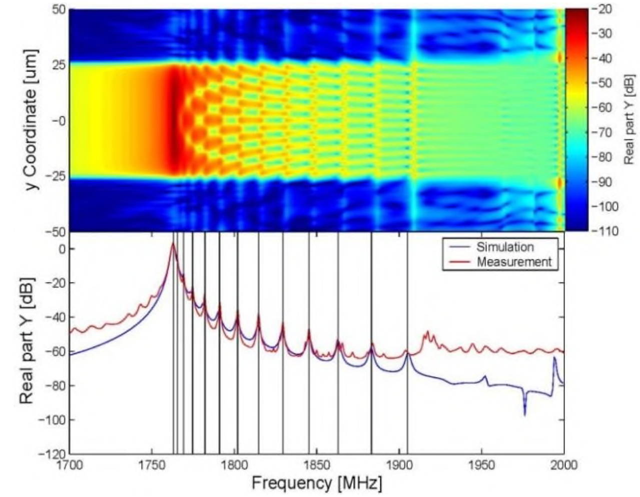

Fig. 3 Field strength over the complete frequency range (top) and conductance frequency response (bottom). Supplementary vertical lines indicate spurious peaks.

$$E^k = \langle e(y)|\psi^k\rangle = \int_{-\frac{A}{2}}^{\frac{A}{2}} e(y)\cdot\psi^k(y)dy, \tag{3}$$

where $e(y)$ and $\psi^k(y)$ are the transversal excitation and mode profile of the kth mode, respectively. Both functions, $e(y)$ and $\psi^k(y)$, are normalized. Since antisymmetric modes are cancelled out, only the symmetric transversal modes are visible in the spectrum. Hence, only the symmetric modes are indicated in Fig. 1.

III. Analysis

We study the effect of 2D periodic patches on electrodes for one port resonators with 5 different periods for the patch and 6 different patch etas. A one-port resonator without patches serves as reference structure. *128°Y-X* $LiNbO_3$ is chosen as a substrate material, where the surface of the substrate is coated with SiO_2. For the electrodes and patches, the same kind of metallization is used. Here, we mainly discuss the analysis of two resonators; one is the reference and the other one is the case with the optimum mode suppression. The comparison is good enough to grasp the principle of mode suppression and the mode development by the periodic array. First we consider the reference structure.

A. One Port Resonator: Reference Structure

Over the entire active aperture, the transversal metallization ratio is homogeneous. Therefore the transversal excitation profile is given by;

$$e = \begin{cases} e_0 & y \in \left[-\frac{A}{2}, \frac{A}{2}\right] \\ 0 & else \end{cases}. \tag{4}$$

However, in general, the excitation profile is frequency dependent and can be obtained from 2D P-matrix computation [11]. In the calculation of mode contributions to admittance, Eq. (3) and (4) are used and the frequency dependency is considered (Fig. 2). As observable in Fig. 2, the decrease of

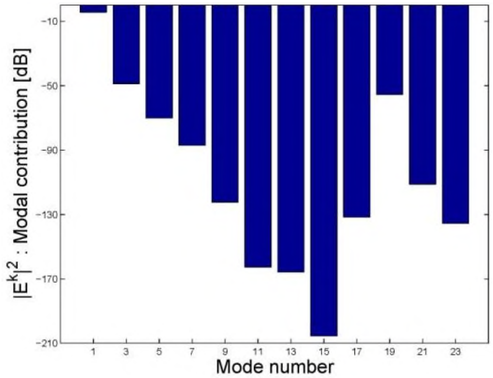

Fig. 4 Transversal mode contribution on spurious peaks. Only symmetric modes are displayed.

the mode contribution only from the 1st to the 2nd symmetric mode is dramatic compared to the higher symmetric modes. Therefore spurious peaks of the higher symmetric modes except for the second being very close to the fundamental mode, are well distinguishable. On the other hand, the simulation based on the 2D P-matrix is capable to compute the field strength. In this model, a unit cell is defined with 2 strips, which then is infinitely cascaded taking into account reflection and diffraction [8], [9], [10]. The field strength over the complete frequency range is visualized in Fig. 3.

Interestingly, in Fig. 3 top, the number of nodes in the field strength increases as the frequency increases. Spurious peaks are located at frequencies, where the number of nodes starts to change. Therefore Fig. 3 provides us with the insight of the mode development over the frequency and the responsible transversal mode for the peaks (Fig. 3 bottom).

B. Resonator with 2D Periodic Array

We now turn to the investigation of a resonator with 11 patches in the active track region. The excitation profile of the resonator with the 2D periodic patches on the electrodes is no longer homogeneous over the entire transversal aperture unlike the reference resonator. Therefore the excitation profile is given by

$$e = \begin{cases} e_0 & y \in \boldsymbol{T} \\ e_1 & y \in \boldsymbol{P} \\ 0 & else \end{cases} , \qquad (5)$$

where $\boldsymbol{T}$ and $\boldsymbol{P}$ are the regular region and the region with patches, respectively. In addition, the velocity profile over the transversal aperture is also not homogeneous owing to the patches. As a result, the mode profile for the kth mode is changed. The contribution of the kth transversal mode to the conductance is computed now by Eq. (3) using Eq. (5) and the new mode profile, $\boldsymbol{\psi_D^k}(\boldsymbol{y})$.

Fig. 4 shows the excitation strengths of the modes. The excitation strength from the 1st symmetric mode to the 11th are larger than the one in Fig. 2, which means the spurious peaks are well suppressed in this region (Fig. 5 bottom). In Fig. 4, the mode contribution from the 9th symmetric mode (17th mode) to the 12th symmetric mode (23 rd mode) is strongly

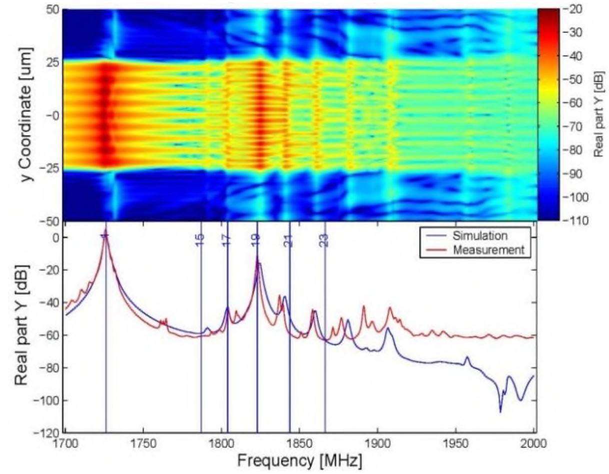

Fig. 5 Field strength over the complete frequency range (top) and frequency response on conductance (bottom).

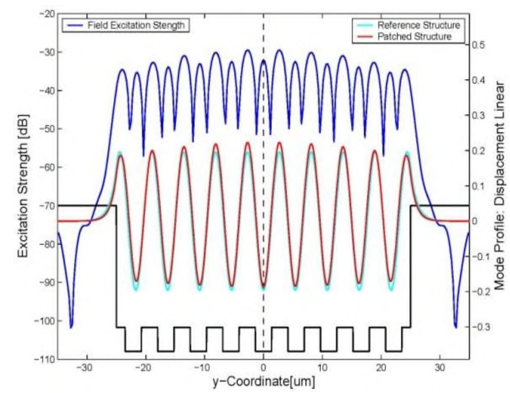

Fig. 6 Field strength for the frequency corresponding to the 19th mode (blue), velocity profile (black) and the 19th mode profiles for reference (cyan) and the structure with patch (red). Each of them is scaled for ease of comparison

increased so that the spurious peaks caused by these modes are observable in the frequency response of conductance (Fig. 5 bottom). Especially the peak on the 19th mode position is very strong in agreement with Fig. 4, where the mode contribution is large.

In Fig. 5 top unlike to Fig. 3 top, up to the resonance frequency of the 15th mode, no change in the field pattern is visible; rather the profile resembles the fundamental mode. This is consistent with a reasonable mode suppression. The spurious peaks appear where the transitions to the next higher modes take place.

In Fig. 6, the field strength and velocity profile of the structure with patches, and the mode profiles for both the reference structure and the structure with patches at the corresponding frequency of 19th mode are respectively plotted over transversal direction. Each of them is respectively scaled in order to make a comparison possible. As can be seen, the mode profile of the structure with patches is somewhat more concentrated in the center of the track than the mode profile of the reference. The reason of the difference is owing to the different boundary condition by the periodic velocity profile. Consequently, the resulting value of the overlap integral by Eq.

(3) increases. The mode responsible for the excitation is the one which has the same number of maxima and minima as the transversal velocity profile produced by the periodic array of the metal patches. This equal periodicity is the reason for the strong spurious peak of the 19^{th} mode. Note that, at each transition point in Fig. 5 top, radiation towards the transversal direction takes place and is especially large for the 19th mode. It is worth noting that the frequency position of the 19^{th} mode agrees well with the one predicted even if neglecting any mode conversion. This may be due to the fact that the mode and reflection profile are very similar and therefore little mode conversion occurs.

C. *Variation of Patch Periodicity*

In order to investigate the effect of patch periodicity on the mode spectrum, the patch length is varied by changing the number of patches from 11 to 19 within the active track. In Fig. 7, the resulting frequency characteristics are plotted. For comparison, the main resonance frequencies, being shifted by the periodic array, are matched to the resonance frequency of the reference structure. For the sake of clarity, a 30dB offset is given on each curve. As the patches on the electrodes influence the boundary condition of the mode profile, the resulting profile is also changed. For the cases presented, the modal contribution of the transversal excitation increases as the number of patches increases. Therefore, as shown in Fig. 7, the higher the number of patches, the worse is the mode suppression. For the worst case, the effect of the patches on the electrodes eventually disappears completely.

IV. CONCLUSIONS

We have fabricated one-port resonators with 2D periodic metal patches on the top of the electrodes. Admittances and field distributions were computed using the 2D P-matrix model. By evaluating the overlap integral of the transversal excitation and mode profile, the excitation strengths of transversal modes were computed. From the analysis of the velocity and the mode profile with the field strength, the transversal mode development and the mechanism of mode suppression are understood.

Resonators with a reasonable number of patches exhibit the second transversal resonance frequency, where the transversal mode and the patch period match. The transversal modes within the frequency band for $k_y = \left[0, \frac{\pi}{P_T}\right]$ are nicely suppressed. In addition, we found that a reasonable patch length should be employed to suppress transversal modes. Otherwise, the contribution of the transversal modes increases which leads to a bad suppression of the corresponding spurious peaks.

By this work, therefore, it is demonstrated that a 2D periodic array can be successfully employed to suppress undesired modes within the frequency band for $k_y = \left[0, \frac{\pi}{P_T}\right]$. The frequency band can be engineered by the pitch of the transversal patch. Alternatively it is also possible to consider other simple periodic structures resulting in a similar waveguiding effect like patches directly on top of the electrodes. Such alternative periodic modulations of the transducer electrodes are presently under investigation and will be discussed elsewhere.

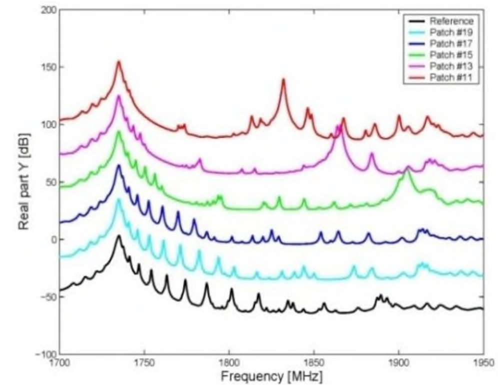

Fig. 7 Frequency dependence of conductance. Patch periodicity is varied by changing the patch number from 11 to 19 within the active track. The main resonance frequencies, which are shifted by the periodic array, are matched to the resonance frequency of the reference resonator. 30dB offset is given on each curve.

ACKNOWLEDGMENT

The authors would like to deliver special thanks to Mr. H. Zottl, Mr. S. Berek, Mr. H. Oeztuerk for the fabrication of samples and the measurement.

REFERENCES

[1] C.C.W. Ruppel, R. Dill, A. Fischerauer, G. Fischerauer, A. Gawlik, J. Machui (1993). SAW devices for consumer communication applications. “Ultrasonics, Ferroelectrics and Frequency Control, IEEE Transactions on”, 40 (5), 438-452.

[2] C. Campbell (1999). “"RF Design", One-port leaky-SAW resonators: building blocks for low-loss RF front-end systems.”

[3] N. Pocksteiner, M. Jungwirth, G. Kovacs, and R. Weigel (2000). Analysis of general planar waveguides with N segments., 1, pp.: 137 - 141 vol.1.

[4] S. Rooth, and A. Ronnekleiv (1996). SAW propagation and reflections in transducers behaving as waveguides in the sense of supporting bound and leaky modes., 1, pp.: 201 -206 vol.1.

[5] M. Mayer, A. Bergmann, G. Kovacs, & K. Wagner (2005). Low loss recursive filters for basestation applications without spurious modes. “IEEE”, 2, pp.: 1061-1064.

[6] M. Solal, J. Gratier, & T. Kook (2009). A SAW resonator with two-dimensional reflectors. “IEEE”, (pp.: 226-231).

[7] Vincent Laude, Mikael Wilm, Sarah Benchabane, and Abdelkrim Khelif. (2005). Full band gap for surface acoustic waves in a piezoelectric phononic crystal. “Phys. Rev. E”, 71, 036607.

[8] M. Mayer, G. Kovacs, A. Bergmann, and K. Wagner (2003). A powerful novel method for the simulation of waveguiding in SAW devices., 1, pp.: 720 - 723 Vol.1.

[9] K. Wagner, M. Mayer, A. Bergmann, and G. Riha (2006). A 2D P-Matrix Model for the Simulation of Waveguiding and Diffraction in SAW Components (Invited)., (pp.: 380-388).

[10] G. Kovacs (2003). A generalised P-matrix model for SAW filters., 1, pp.: 707 - 710 Vol.1.

[11] M. Mayer, A. Bergmann, K. Wagner, M. Schemies, T. Telgmann, and A. Glas (2004). Low resistance quartz resonators for automotive applications without spurious modes. “IEEE”, 2, pp.: 1326-1329.